https://doi.org/10.48048/tis.2025.9466

IgY Anti-N SARS CoV2-Conjugated Gold Nanoparticles Production for Lateral Flow Biosensor-Based Diagnostics

Idar Idar[1,2], Muhammad Yusuf[3,4], Jamaludin Al Anshori[5] and Toto Subroto[4,5,*]

[1]Biotechnology Study Program, Graduate School, Universitas Padjadjaran, Jawa Barat 40132, Indonesia
[2]Faculty of Pharmacy, Universitas Bhakti Kencana, Jawa Barat 40614, Indonesia
[3]Vocational Chemical Industry Technology Program, Faculty of Mathematics and Natural Sciences, Universitas Padjajaran, Sumedang 45363, Indonesia
[4]Research Center for Molecular Biotechnology and Bioinformatics, Universitas Padjadjaran, Bandung 40132, Indonesia
[5]Department of Chemistry, Faculty of Mathematics and Natural Sciences, Universitas Padjajaran, Sumedang 45363, Indonesia

([*]Corresponding author's e-mail: t.subroto@unpad.ac.id)

Received: 7 December 2024, Revised: 26 December 2024, Accepted: 2 January 2025, Published: 10 February 2025

Abstract

Although the number of COVID-19 cases is decreasing, the virus continues circulating, necessitating ongoing detection efforts. This is particularly important because COVID-19 symptoms like fever can resemble those of other tropical diseases like dengue fever. Lateral Flow Strip Biosensors (LFSB) offer a rapid and cost-effective testing method to address this issue. A crucial factor influencing the sensitivity and specificity of LFSB is the conjugate, which consists of a detection antibody and a visualization agent. Anti-N-SARS-CoV-2 IgY can be utilized as the detection antibody. This antibody was produced by immunizing chickens with a stable antigen derived from the SARS-CoV-2 virus, specifically the SARS-CoV-2 nucleocapsid protein (N-SARS-CoV-2). Gold nanoparticles serve as the visualization agent, enabling visual readings of the LFSB without additional equipment. The size of the gold nanoparticles affects their surface area and the resulting color, affecting the sensitivity of the LFSB. While various sizes of gold nanoparticles are available commercially, they tend to be quite costly, affecting the production expenses of the LFSB. Therefore, this study aims to develop LFSB conjugates for SARS-CoV-2 detection by synthesizing gold nanoparticles of different sizes and conjugating them with IgY anti-N-SARS-CoV-2. The gold nanoparticles were synthesized using the Turkevich-Seed Growth method, which allows for variations in size within a single synthesis process and uses non-toxic materials. The synthesized gold nanoparticles were characterized using a spectrophotometer, and their sizes were analyzed with a particle size analyzer. Subsequently, they were conjugated with anti-N-SARS-CoV-2 IgY via a passive conjugation method. The conjugates were characterized based on maximum wavelength shifts, and their aggregation parameters and functionality were tested using a half-strip spot test. This research demonstrates that gold nanoparticles of 63.9 nm are the most suitable for conjugation with anti-N-SARS-CoV-2 IgY.

Keywords: Lateral flow, Diagnostic, Gold nanoparticle, Conjugation, IgY, Synthesis

Introduction

Although COVID-19 has passed, the virus continues circulating, making it essential to detect this disease. This is particularly important since the symptoms (e.g. fever) of COVID-19 can be similar to various endemic diseases found in tropical regions, such as dengue fever [1-3]. Test strips or Lateral Flow Strip Biosensor (LFSB) remain a fast and economical option for detection. LFSB meets the WHO ASSURED criteria: Affordable, sensitive, specific, user-friendly, rapid, robust, equipment-free, and deliverable to end-

users [4]. Numerous LFSBs utilizing nanotechnology have been developed. This type of point-of-care testing is particularly advantageous in developing countries with limited laboratory equipment. With LFSBs, there is no need to send samples for testing, allowing for cost reduction and immediate access to test results [5,6]. Additionally, this rapid detection aims to provide a quick and accurate diagnosis to help mitigate the severity of the disease.

The working principle of LFSB (Lateral Flow Strip Bioassay) is based on binding the target analyte in the sample to a conjugate. This binding leads to the accumulation of particles on both the test and control lines, forming 2 red lines. Conversely, if the target analyte is absent, particles will only accumulate on the control line, producing a single red line [7,8]. The conjugate plays a crucial role in determining the validity of the LFSB [8]. This validity is assessed through 2 key parameters: Specificity and sensitivity. Specificity (or selectivity) refers to detecting a specific analyte amidst a mixture of different analytes. At the same time, sensitivity indicates the minimum amount of analyte that can be accurately detected [9,10]. The conjugate comprises a detection antibody labeled with a visualizing agent that specifically binds to the analyte. Therefore, careful consideration is necessary in selecting, designing, and producing detection antibodies and visualizing agents to ensure accurate results.

As a detection antibody, we can utilize IgY, which is an antibody produced by birds. The nucleocapsid protein of SARS-CoV-2 (N-SARS-CoV-2) is a stable antigen associated with the SARS-CoV-2 virus. This protein can immunize birds, leading to the production of anti-N-SARS-CoV-2 IgY [11]. One significant advantage of using IgY is that it can be obtained in large quantities, as it is primarily found in chicken egg yolk. However, using IgY as a detection antibody in commercial LFSB is still relatively uncommon, presenting a significant opportunity for development. For clarity, this study will refer to anti-N-SARS-CoV-2 IgY simply as IgY.

The other component of the conjugate is the visualizing agent. Gold nanoparticles are commonly utilized as visualizing agents in LFSB. These nanoparticles range in size from 1 to 100 nm [12] and possess a distinct color that allows for visual reading of the LFSB without additional tools. Several studies indicate that the size of gold nanoparticles can affect the sensitivity of LFSB. Based on this, the size of the gold nanoparticles used in LFSB varies according to specific requirements. For example, 40 nm is used for detecting hepatitis B [13], 14 nm for tuberculosis [14], 20 nm for Gumboro disease [15], and 40 nm for fumonisins (mycotoxins) [16]. For the receptor-binding domain (RBD) of SARS-CoV-2, a size of 20 nm is employed [17], while a size of 14 nm is used for conjugation with streptavidin [18]. Even now, a combination of nanoparticles and enzymes is being developed as a visualizing agent to strengthen the signal produced [19].

The synthesis of gold nanoparticles generally involves 2 main approaches: Top-down and bottom-up methods. The top-down approach entails decomposing bulk gold metal into nano-sized particles, while the bottom-up approach focuses on assembling atoms or molecules to form nanoparticles [20]. These approaches can be classified into physical, chemical, and biological methods. Among these, the Turkevich method is the most commonly used chemical synthesis technique, accounting for approximately 60 % of gold nanoparticle synthesis [21,22]. This method is based on reduction reactions and consists of 3 key components: Metal precursors (such as metal salts), reducing agents (including trisodium citrate, hydrazine, ascorbic acid, and sodium borohydride), and capping/stabilizing agents (like phosphorus ligands, trisodium citrate, cetyltrimethylammonium bromide (CTAB), chitosan, surfactants, and various polymers) [20,23]. The Turkevich method typically yields nanoparticles measuring between 20 - 40 nm. The seed growth method can produce larger gold nanoparticles, allowing a size range from 10 to 300 nm [24-27].

Currently, the domestic industry produces various lateral flow-based rapid diagnostics for detecting different diseases. However, most components, including the conjugate, are still imported. By producing our conjugate, we can significantly reduce the production costs of these rapid tests.

In summary, this research will focus on synthesizing gold nanoparticles using the Turkevich-Seed Growth method. This method has several advantages, including obtaining various sizes of nanoparticles simultaneously in a single reaction and using non-toxic reagents. The resulting nanoparticles will be characterized after conjugation with IgY using

the passive conjugation method to determine the most suitable synthesized nanoparticles. A passive conjugation method will create gold nanoparticle-conjugated immunoglobulin Y (IgY). This method relies on hydrophobic interactions, ionic interactions, and dative bonds formed between the surface charges of gold nanoparticles and antibodies. Compared to the covalent conjugation method, the passive approach is more cost-effective because it does not require a linker compound. However, a drawback of this method is the randomness in antibody attachment orientations. This issue can be mitigated by carefully controlling the pH of the components involved, namely the gold nanoparticles and antibodies.

Materials and methods

IgY purification

Purification of IgY was carried out using a chromatographic method; the stationary phase was butyl toyopearl 650 M, and the eluant was potassium sulfate in trisodium phosphate [11].

Gold nanoparticle synthesis and characterization

Gold nanoparticles synthesis

The synthesis of gold nanoparticles was performed based on research by Bastús *et al.* [24]; Ziegler and Eychmüller [27], with several modifications. Fifty mL of 2.2 mM trisodium citrate was added to a 3-neck reflux flask, heated, and stirred until boiling. Then, 1 mL of 8.4 mM chloroauric acid was introduced, resulting in a color change after approximately 10 min. Two mL of this mixture were aliquoted into a dark bottle labeled "seed", cooled on ice, and stored at 4 °C for later use. The solution's temperature was lowered and maintained at about 90 °C. Another 1 mL of chloroauric acid was added and heated for 25 min, followed by a second addition of the same volume and heating for 25 min. After that, 19 mL of the solution was aliquoted into a dark bottle, cooled on ice, labeled G0, and stored at 4 °C. Subsequently, 17 mL of hot demineralized water and 2 mL of 22.35 mM trisodium citrate were added. This cycle was repeated 12 times, yielding 13 variations of gold nanoparticles labeled G0 to G12. The steps were depicted more clearly in the gold nanoparticle synthesis diagram in **Figure S1** of the supplement.

Gold nanoparticles characterization

Characterization of gold nanoparticles involves measuring their spectral properties, particle size, and polydispersity index (PDI). The spectra of the synthesized gold nanoparticles were recorded using a UV-1800 SHIMADZU SPECTROPHOTOMETER over a wavelength range of 400 to 800 nm. The gold nanoparticles' particle size and PDI were also assessed using a HORIBA SZ-100 particle size analyzer.

IgY-gold nanoparticles conjugation

Gold nanoparticles pH optimization

The stability of AuNPs to pH was assessed by diluting each AuNP in a ratio of 1:1 with trizma buffer at 3 different pH levels: 7, 8, and 9. Then, 130 µL of each were taken and put into a microplate well, and their spectra were scanned by a microplate reader, MULTISKAN SKYHIGH, at 400 to 800 nm in wavelength.

IgY concentration optimization

For every 100 µL of synthesized gold nanoparticles (AuNP), 10 µL of IgY was added at varying concentrations of 40, 60, 80, 100, 150, 175, and 200 µg/mL. The pH was adjusted using Trizma buffer to reach the optimum level. The mixture was then incubated at room temperature for 30 min, with occasional shaking. After incubation, 20 µL of 10 % NaCl was added, and the solution was allowed to rest for 5 min. The resulting spectral pattern was measured using a microplate reader over a 400 to 800 nm wavelength range.

Conjugation

One mL of each synthesized gold nanoparticle (AuNP) suspension was taken, and the pH was adjusted to the optimum level using a 0.3 M K_2CO_3 solution. Subsequently, 100 µL of immunoglobulin Y (IgY) dissolved in a 10 mM Trizma buffer was added. Both the IgY concentration and pH used are the results of optimization. The solution was stirred using a rotating mixer at 35 rpm for 30 min. Then, centrifugation was performed at 14,000 rpm and 4 °C for 20 min. The resulting pellet was resuspended in a 2 mM Trizma buffer at the optimum pH. Bovine serum albumin (BSA) was added to achieve a final concentration of 1 %, and the mixture was stirred at 35 rpm for another 30 min.

Afterward, centrifugation was repeated at 14,000 rpm and 4 °C for 20 min. The final pellet was resuspended with the diluent conjugate. The spectrum pattern was measured using a microplate reader across a 400 - 800 nm wavelength range. The conjugate was then stored in a dark container. Conjugation was also performed on 40 nm commercial gold nanoparticles (*nanoflow*) using the same method.

Conjugate characterization

Spectra analysis

The spectra of gold nanoparticles resulting from the synthesis were measured by spectrophotometer, UV-1800 SHIMADZU SPECTROPHOTOMETER, at 400 to 800 nm in wavelength.

Half-strip spot test

A half strip was used to prepare both test and control spots. It was done by dispensing IgG anti-SARS-CoV-2 (1 mg/mL) and goat IgG anti-chicken (1 mg/mL) onto a nitrocellulose membrane, then dried at 37 °C for approximately 2 h. Once dry, the nitrocellulose membrane was attached to a PVC backing card and overlapped with an absorbent pad.

Then, each conjugate to be tested was prepared by combining 49 µL of conjugate, 1 µL N-SARS-CoV-2 protein 1 µg/mL, and Tween-20 at 0.05 % in final concentration. This solution was then placed into the wells of a microplate. Next, the prepared half strip was inserted into the microplate containing the conjugate. The solution was allowed to flow over the half strip for 15 min, after which the formation of spots was observed on the control and test areas.

To estimate the sensitivity of the conjugate, the area of the spot produced on the test spot was calculated using ImageJ software. Subsequently, the area was plotted on a graph in Excel.

Successful half-strip assay requires various optimizations, including the concentration and type of blocking agent (e.g., BSA), the detergent (e.g., Tween-20), and the buffer used for conjugation.

Results and discussion

IgY purification

IgY, an anti-N-SARS CoV2 protein obtained from chicken egg yolks immunized with the N-SARS CoV2 protein, was isolated and purified using PEG-6000 precipitation and hydrophobic column chromatography with Butyl Toyopearl 650 M. The purified IgY has a protein content of 69 mg/mL.

Gold nanoparticle synthesis and characterization

The results from the size characterization revealed that the gold nanoparticle samples, designated from G0 to G12, exhibited progressively larger sizes. This indicates that the synthesis of gold nanoparticles using the Seed Growth method produces nanoparticles that increase in size with the number of synthesis cycles (**Figure 2**).

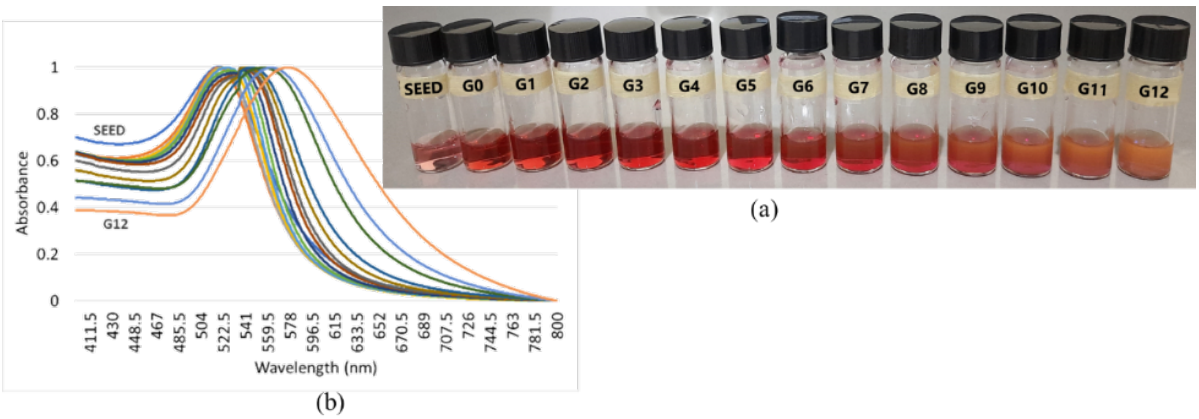

Figure 1 Gold nanoparticles were synthesized using the seed growth method (a) and their normalized spectrum patterns (b). The results of the synthesis were labeled as seed (), G0 (), G1 (), G2 (), G3 (), G4 (), G5 (), G6 (), G7 (), G8 (), G9 (), G10 (), G11 (), and G12 ().

	Seed	G0	G1
	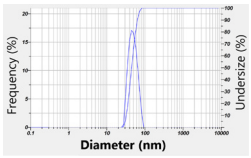	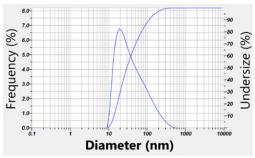	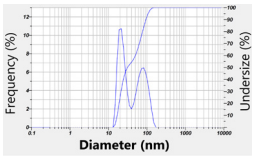
Particle size (nm)	37.2 ± 2.1	30.5 ± 3.1	32.7 ± 0.5
PDI	0.666 ± 0.12	0.466 ± 0.06	0.401 ± 0.04

	G2	G3	G4
	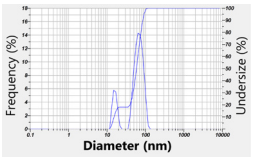	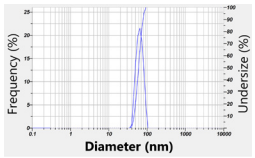	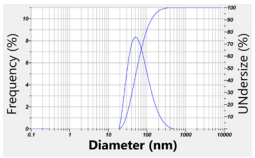
Particle size (nm)	44.1 ± 1.4	46.3 ± 0.9	55.0 ± 1.1
PDI	0.418 ± 0.01	0.370 ± 0.03	0.287 ± 0.04

	G5	G6	G7
	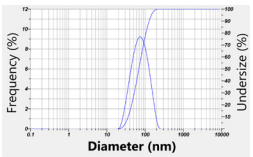	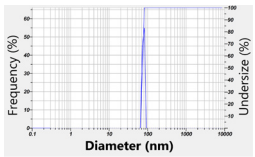	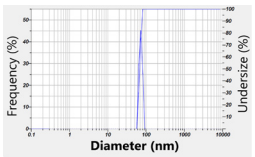
Particle size (nm)	63.9 ± 1.0	64.1 ± 0.5	59.9 ± 0.6
PDI	0.226 ± 0.02	0.490 ± 0.02	0.497 ± 0.04

	G8	G9	G10
	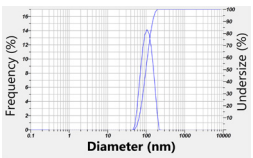	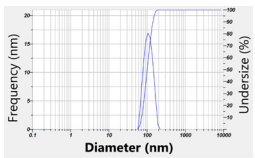	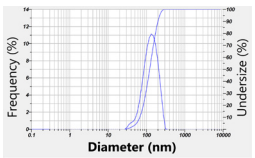
Particle size (nm)	86.1 ± 1.9	91.5 ± 1.1	111.4 ± 4.2
PDI	0.232 ± 0.02	0.248 ± 0.03	0.170 ± 0.04

	G11	G12
	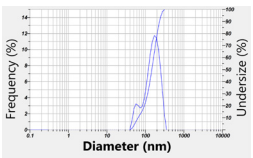	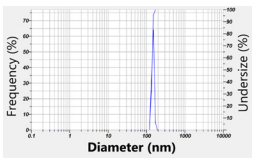
Particle size (nm)	127.9 ± 8.5	128.2 ± 3.0
PDI	0.251 ± 0.08	0.343 ± 0.04

Figure 2 The size of the gold nanoparticles produced through synthesis was measured using a Particle Size Analyzer and their polydispersity index (PDI).

A seed was synthesized using the seed growth method described by Bastús *et al*. [24]. This initial seed was then subjected to 13 synthesis cycles, resulting in the production of 14 gold nanoparticles, referred to as seed, G0 - G12 (**Figure 1(a)**). Each nanoparticle generates an absorption spectrum that displays a typical

pattern for nanoparticles. It is characterized by the highest absorption in the wavelength range of 500 - 600 nm, and absorption at wavelengths greater than 600 nm is lower than at wavelengths below 500 nm.

The normalization of the spectrum pattern for the synthesized nanoparticles, as shown in **Figure 1(b)**, indicates a shift in the maximum wavelength from the seed (far left) to G12 (far right), progressively moving to larger wavelengths. This shift aligns with the observable changes in the color of the samples, transitioning from pink and burgundy to orange, as illustrated in **Figure 1(a)**.

According to ISO 22412:2017 on particle size analysis utilizing the Dynamic Light Scattering (DLS) principle, a nanoparticle was classified as monodisperse if its polydispersity index (PDI) value was less than 0.05 [28]. Conversely, a PDI value greater than 0.7 categorizes the nanoparticle as polydisperse. In this case, the synthesized gold nanoparticles have a PI value of less than 0.5, which indicates relatively good dispersity, even though they do not reach the monodisperse classification (**Figure 2**).

Figure 2 illustrates that the pattern of increasing nanoparticle size becomes clearly defined starting from G1. Nanoparticles are defined as particles with sizes ranging from 1 to 100 nm [12]; therefore, the final nanoparticle selected for this research was G10. Thus, the nanoparticles from G1 to G10 will be utilized to produce the IgY-conjugated nanoparticle.

IgY-gold nanoparticles conjugation

The stability of the conjugate components, IgY, and the synthesized gold nanoparticles played a crucial role in the bioconjugation reaction. pH was a factor in the buffer used during the conjugation process, significantly impacting stability. IgY was stable over a wide pH range, specifically between pH 3 and pH 11 [29], eliminating the need for pH stability testing for IgY. In contrast, gold nanoparticles were charged particles, making their stability highly dependent on pH. Therefore, assessing the environmental pH stability of gold nanoparticles was essential.

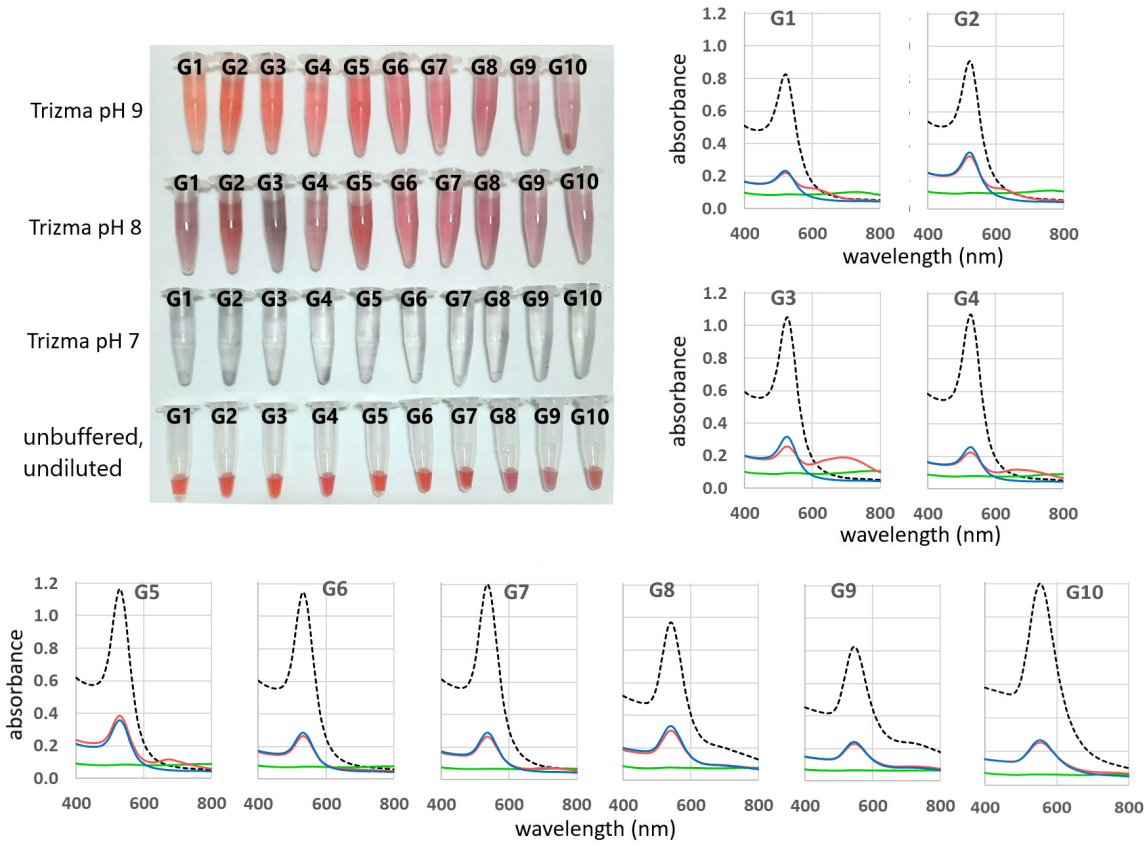

Figure 3 The color and spectrum pattern of each synthesized gold nanoparticle diluted in Trizma buffer at pH 7 (—), pH 8 (—), and pH 9 (—) compared to its unbuffered gold nanoparticle (.....).

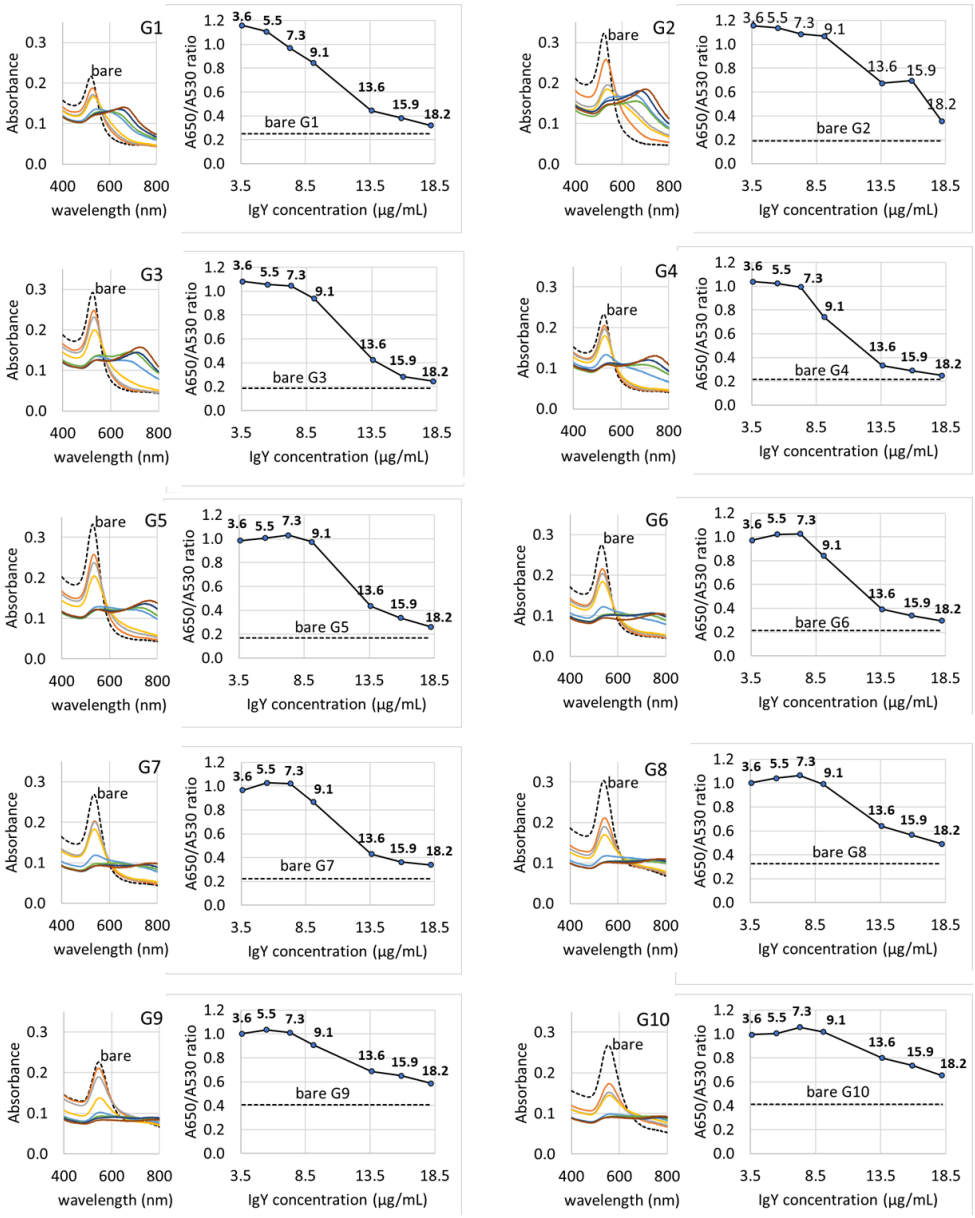

Figure 4 Characterization of the synthesized gold nanoparticle by flocculation assay at a pH 9 Trizma buffer, conjugated with IgY at final concentrations of 3.6, 5.5, 7.3, 9.1, 13.6, 15.9, and 18.2 µg/mL compared to bare gold nanoparticles, including spectral patterns G1 - G10, as well as its aggregation parameters (absorption ratio at 650 nm and 530 nm).

This research performed a stability test of the synthesized gold nanoparticles by diluting them in Trizma buffer at pH levels 7, 8, and 9. The results indicated that pH 9 was the most suitable environmental pH for the synthesized nanoparticles. As shown in **Figure 3**, at Trizma buffer pH 7, the gold nanoparticles (G1 - G10) became clear, losing their color compared to the unbuffered gold nanoparticles. This observation was consistent with the spectral pattern, which flattened, as indicated by the green line in the absorption versus wavelength graph (**Figure 3**).

When comparing the stability of gold nanoparticles in Trizma buffer at pH 8 to those at pH 9, it was evident that pH 9 was the optimal condition. The gold nanoparticles retained a relatively red color at this pH, similar to the unbuffered gold nanoparticles. Additionally, all the spectral patterns of the synthesized gold nanoparticles (G1 - G10) at pH 9 (represented by the blue line) matched the spectrum pattern of the unbuffered gold nanoparticles (**Figure 3**).

Another crucial factor in the successful production of this conjugate was the accuracy of the IgY concentration, making it necessary to optimize this

concentration. The optimization was tested using a flocculation assay. In principle, adding salt to the gold nanoparticles causes them to aggregate, so the correct IgY concentration was essential to adequately cover the surface of the gold nanoparticles.

In this study, the flocculation assay was conducted using IgY concentrations of 40, 60, 80, 100, 150, 175, and 200 µg/mL. When converted to the final concentration of IgY in the test solution, the resulting concentrations were 3.6, 5.5, 7.3, 9.1, 13.6, 15.9, and 18.2 µg/mL, respectively. The absorbance graph indicated that IgY concentrations of 13.6, 15.9, and 18.2 µg/mL produced a spectral pattern for the gold nanoparticles similar to that of bare gold nanoparticles. In contrast, adding IgY at concentrations less than 9.1 µg/mL resulted in a different spectral pattern.

This finding was supported by the graph plotting the ratio of A650/A530 against IgY concentration. By calculating the absorbance ratio at 650 nm to that at 530 nm, it was determined that a higher ratio value indicates a greater formation of gold nanoparticle aggregates. Consistent with the absorption versus wavelength graph, the A650/A530 versus IgY concentration graph also demonstrates that the use of IgY at final concentrations of 13.6, 15.9, and 18.2 µg/mL resulted in low ratio values, closely resembling those of bare gold nanoparticles (**Figure 4**).

Based on these results, an IgY concentration of 13.6 µg/mL (derived from an addition of 175 µg/mL of IgY) was chosen for efficiency and cost-effectiveness in conjugate production. Conjugation of the IgY with the synthesized nanoparticles (G1 - G10) was conducted passively, following the procedures outlined in the materials and methods. This process resulted in the production of 10 conjugates, which were subsequently characterized.

Conjugate characterization

Spectra analysis

Spectrum patterns and spot tests characterized the IgY conjugates with G1 to G10. The spectrum analysis indicated that G5 - G7 are the most suitable gold nanoparticles for conjugation. This conclusion was supported by the conjugate spectrum pattern (represented by the black line), which closely resembles the spectrum pattern of the unconjugated nanoparticles (shown by the dashed black line) (**Figure 5**). Among the 3 nanoparticle conjugates—G5 - G7—it was determined that G5 was the best candidate for conjugation with IgY. This was based on the narrowest maximum wavelength shift and the stability of the conjugates. Additionally, data revealed that G5 had the lowest aggregation parameter values among the conjugates of G5 - G7 (**Table 1**).

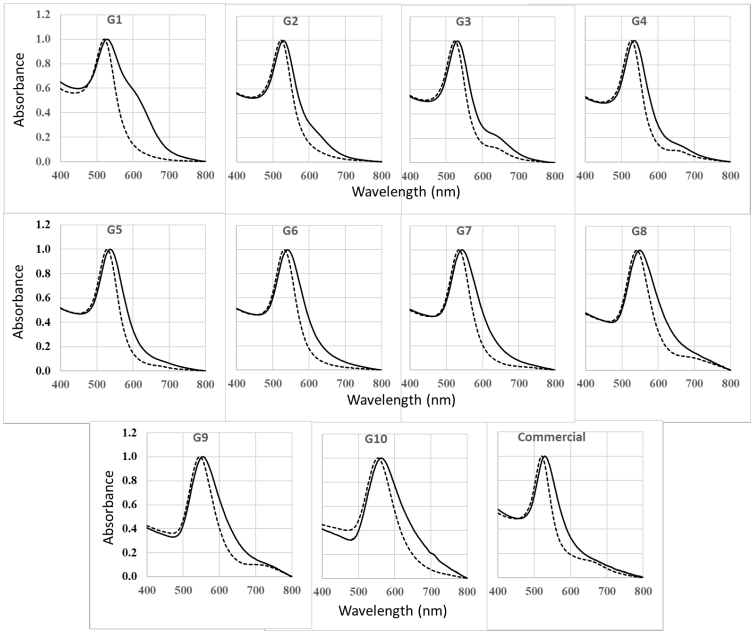

Figure 5 The normalized spectrum patterns of synthesized gold nanoparticles (G1 - G10), both IgY-conjugated (▬) and unconjugated (▪▪▪▪), were compared to the spectrum patterns of commercial gold nanoparticles.

Table 1 The maximum wavelength shift and aggregation parameter of IgY-conjugated synthesized gold nanoparticles (G1 - G10) compared to those of IgY-conjugated commercial gold nanoparticles.

Gold nanoparticles	Δλmax (λmax conjugated - λmax unconjugated)	Conjugated aggregation parameter (A650/A530)
G1	7	0.40
G2	7	0.20
G3	8	0.26
G4	11	0.22
G5	8	0.20
G6	8	0.25
G7	9	0.31
G8	8	0.51
G9	9	0.61
G10	8	0.77
Commercial	8	0.45

Half-strip spot test

A half-strip spot test was conducted to determine whether the conjugate could effectively recognize the target protein, N-SARS-CoV-2. IgG anti-chicken was applied to the control spot on the membrane, while IgG anti-N-SARS-CoV-2 was used on the test spot. Each conjugate combined with N-SARS-CoV-2 protein as a test sample was compared to the conjugate without adding N-SARS-CoV-2 protein, which served as a negative control (**Figure 6**).

The qualitative results from the conjugate test on half strips indicated that all conjugates could detect the presence of the N-SARS CoV2 protein at a concentration of 1 ng. However, the thickness of the spots varied. This concentration of 1 ng was derived from 1 µL of N-SARS CoV2 protein at a concentration of 1 µg/mL, which was used as the test sample. ImageJ software analysis of the spot areas revealed that the G5 conjugate, which utilized 63.9 nm gold nanoparticles, produced the thickest spot. This suggests that the G5 conjugate demonstrated the highest sensitivity compared to other nanoparticles, including the commercial 40 nm nanoparticles. The graph of the area of the spot was detailed in the supplement.

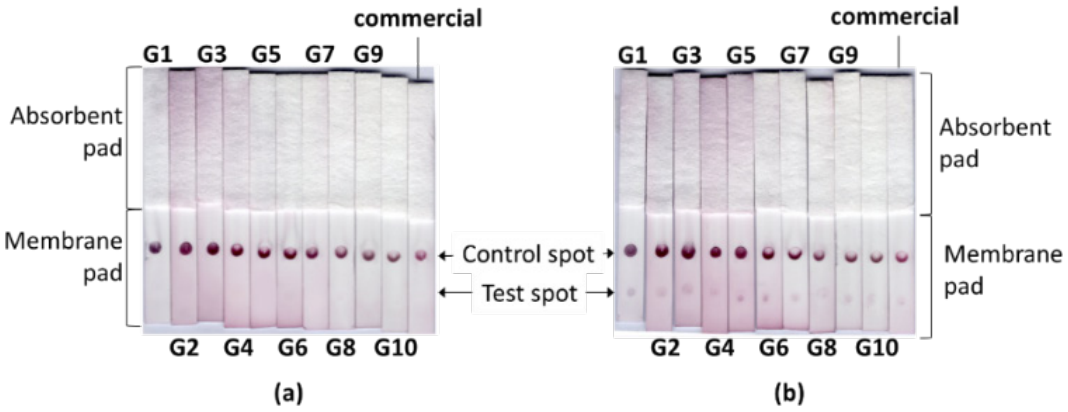

Figure 6 Half-strip spot test results comparing IgY-conjugated synthetic gold nanoparticles (G1 - G10) with commercial nanoparticles, with the N-SARS-CoV-2 protein as the test sample (b) and without the N-SARS-CoV-2 protein as negative control (a). Anti-chicken IgG was applied to the control spot, and anti-N-SARS-CoV-2 IgG was applied to the test spot.

Based on spectral analysis data, maximum wavelength shift, aggregation parameters, and half-strip assays, it was concluded that the G5 conjugate with 63.9 nm gold nanoparticles was the most suitable candidate for use in the lateral flow component.

Conclusions

Based on the findings of this research, it can be concluded that synthesizing gold nanoparticles using the seed-growth method results in an increase in particle size as the number of synthesis cycles rises. The study identified nanoparticles measuring 63.9 nm as the most effective for conjugation with antibodies, specifically IgY anti-N SARS-CoV-2.

To optimize the resulting nanoparticles in size, shape, and reproducibility, it is essential to standardize the synthesis equipment, particularly the reflux system. Standardized equipment allows precise control over parameters influencing synthesis reactions, such as temperature and stirring speed. This precision is crucial for producing gold nanoparticles on a large scale.

Further optimization and testing steps are necessary to develop these conjugates into a functional diagnostic tool. These include the ¾ strip test for real matrices and the full strip test for clinical validation on actual samples. This conjugate is essential, especially considering antibodies and gold nanoparticles are expensive components. Calculations indicate that self-synthesized gold nanoparticles are more economical than commercial ones (**Table S1** in the Supplement), suggesting a strong potential for scaling up production.

Acknowledgments

The authors thank the PMDSU research program for fiscal year 2024. Directorate of Research, Technology and Community Service, Directorate General of Higher Education, Research and Technology, Ministry of Education, Culture, Research and Technology Fiscal Year 2024 number SP DIPA-023.17.1.690523/2024 1st revision dated 4 February 2024.

References

[1] S Khan, SMF Akbar and A Nishizono. Co-existence of a pandemic (SARS-CoV-2) and an epidemic (Dengue virus) at some focal points in Southeast Asia: Pathogenic importance, preparedness, and strategy of tackling. *The Lancet Regional Health - Southeast Asia* 2022; **4**, 100046.

[2] P Hariadi, D Lokida, AM Naysilla, N Lukman, H Kosasih, Y Mardian, G Andru, I Pertiwi, RI Sugiyono, AA Pradana, G Salim, DP Butar-Butar, CY Lau and M Karyana. Coinfection with SARS-CoV-2 and dengue virus: A case report highlighting diagnostic challenges. *Frontiers in Tropical Diseases* 2022; **3**, 801276.

[3] GN Malavige, C Jeewandara and GS Ogg. Dengue and COVID-19: Two sides of the same coin. *Journal of Biomedical Science* 2022; **29(1)**, 48.

[4] HR Boehringer and BJ O'Farrell. Lateral flow assays in infectious disease diagnosis. *Clinical Chemistry* 2021; **68(1)**, 52-58.

[5] OI Guliy and LA Dykman. Gold nanoparticle-based lateral-flow immunochromatographic biosensing assays for the diagnosis of infections. *Biosensors and Bioelectronics: X* 2024; **17**, 100457.

[6] LN Thwala, SC Ndlovu, KT Mpofu, MY Lugongolo and P Mthunzi-Kufa. Nanotechnology-based diagnostics for diseases prevalent in developing countries: Current advances in point-of-care tests. *Nanomaterials* 2023; **13(7)**, 1247.

[7] J Budd, BS Miller, NE Weckman, D Cherkaoui, D Huang, AT Decruz, N Fongwen, GR Han, M Broto, CS Estcourt, J Gibbs, D Pillay, P Sonnenberg, R Meurant, MR Thomas, N Keegan, MM Stevens, E Nastouli, EJ Topol, E Nastouli, EJ Topol, AM Johnson, …, RA McKendry. Lateral flow test engineering and lessons learned from COVID-19. *Nature Reviews Bioengineering* 2023; **1**, 13-31.

[8] C Parolo, A Sena-Torralba, JF Bergua, E Calucho, C Fuentes-Chust, L Hu, L Rivas, R Álvarez-Diduk, EP Nguyen, S Cinti, D Quesada-González and A Merkoçi. Tutorial: Design and fabrication of nanoparticle-based lateral-flow immunoassays. *Nature Protocols* 2020; **15(12)**, 3788-3816.

[9] AK Akobeng. Understanding diagnostic tests 1: Sensitivity, specificity and predictive values. *Acta Paediatrica* 2007; **96(3)**, 338-341.

[10] V Naresh and N Lee. A review on biosensors and recent development of nanostructured materials-enabled biosensors. *Sensors* 2021; **21(4)**, 1109.

[11] I Idar, M Yusuf, JA Anshori and T Subroto. Purification of IgY Anti-SARS-CoV-2-Chicken Nucleocapsid and elimination of its low-temperature storage-induced aggregates. *Trends in Sciences* 2024; **21(5)**, 7649.

[12] RK Goyal. *Nanomaterials and nanocomposites*. Synthesis, properties, characterization techniques, and applications. CRC Press, Boca Raton, Florida, 2018.

[13] DS Kim, YT Kim, SB Hong, J Kim, NS Huh, MK Lee, SJ Lee, BI Kim, IS Kim, YS Huh and BG Choi. Development of lateral flow assay based on size-controlled gold nanoparticles for detection of hepatitis B surface antigen. *Sensors* 2016; **16(12)**, 2154.

[14] PP Seele, B Dyan, A Skepu, C Maserumule and NRS Sibuyi. Development of gold-nanoparticle-based lateral flow immunoassays for rapid detection of TB ESAT-6 and CFP-10. *Biosensors* 2023; **13(3)**, 354.

[15] S Syahruni, YW Hartati, M Yusuf, S Kusumawardani, IWT Wibawan, W Arnafia, G Sibit and T Subroto. Development of lateral flow assay based on anti-IBDV IgY for the rapid detection of Gumboro disease in poultry. *Journal of Virological Methods* 2021; **291**, 114065.

[16] TV Tran, BN Do, TPT Nguyen, TT Tran, SC Tran, BV Nguyen, CV Nguyen and HQ Le. Development of an IgY-based lateral flow immunoassay for detection of fumonisin B in maize. *F1000Research* 2019; **8**, 1042.

[17] D Prakashan, NS Shrikrishna, M Byakodi, K Nagamani and S Gandhi. Gold nanoparticle conjugate-based lateral flow immunoassay (LFIA) for rapid detection of RBD antigen of SARS-CoV-2 in clinical samples using a smartphone-based application. *Journal of Medical Virology* 2023; **95(1)**, e28416.

[18] R D'Agata, P Palladino and G Spoto. Streptavidin-coated gold nanoparticles: Critical role of oligonucleotides on stability and fractal aggregation. *Beilstein Journal of Nanotechnology* 2017; **8**, 1-11.

[19] H Jie, Y Wang, M Zhao, X Wang, Z Wang, L Zeng, X Cao, T Xu, F Xia and Q Liu. Automatic ultrasensitive lateral flow immunoassay based on a color-enhanced signal amplification strategy. *Biosens & Bioelectronics* 2024; **256**, 116262.

[20] AEF Oliveira, AC Pereira, MAC Resende and LF Ferreira. Gold nanoparticles: A didactic step-by-step of the synthesis using the turkevich method, mechanisms, and characterizations. *Analytica* 2023; **4(2)**, 250-263.

[21] M Wuithschick, A Birnbaum, S Witte, M Sztucki, U Vainio, N Pinna, K Rademann, F Emmerling, R Kraehnert and J Polte. Turkevich in new robes: Key questions answered for the most common gold nanoparticle synthesis. *ACS Nano* 2015; **9(7)**, 7052-7071.

[22] MA Dheyab, AA Aziz, PM Khaniabadi, MS Jameel, N Oladzadabbasabadi, SA Mohammed, RS Abdullah and B Mehrdel. Monodisperse gold nanoparticles: A review on synthesis and their application in modern medicine. *International Journal of Molecular Sciences* 2022; **23(13)**, 7400.

[23] CDD Souza, BR Nogueira and MECM Rostelato. Review of the methodologies used in the synthesis gold nanoparticles by chemical reduction. *Journal of Alloys and Comppounds* 2019; **798**, 714-740.

[24] NG Bastús, J Comenge and V Puntes. Kinetically controlled seeded growth synthesis of citrate-stabilized gold nanoparticles of up to 200 nm: Size focusing versus ostwald ripening. *Langmuir* 2011; **27(17)**, 11098-11105.

[25] Q Yao, X Yuan, V Fung, Y Yu, DT Leong, DE Jiang and J Xie. Understanding seed-mediated growth of gold nanoclusters at molecular level. *Nature Communications* 2017; **8(1)**, 927.

[26] K Liu, Z He, JF Curtin, HJ Byrne and F Tian. A novel, rapid, seedless, in situ synthesis method of shape and size controllable gold nanoparticles using phosphates. *Scientific Reports* 2019; **9**, 7421.

[27] C Ziegler and A Eychmüller. Seeded growth synthesis of uniform gold nanoparticles with diameters of 15 - 300 nm. *Journal of Physical Chemistry C* 2011; **115(11)**, 4502-4506.

[28] The International Organization for Standardization. *ISO 22412:2017: Particle size analysis - Dynamic light scattering (DLS)*. The International Organization for Standardization, Geneva, Switzerland, 2017.

[29] JMPDL Lastra, V Baca-González, P Asensio-Calavia, S González-Acosta and A Morales-Delanuez. Can immunization of hens provide oral-based therapeutics against covid-19? *Vaccines* 2020; **8(3)**, 486.

Supplementary material

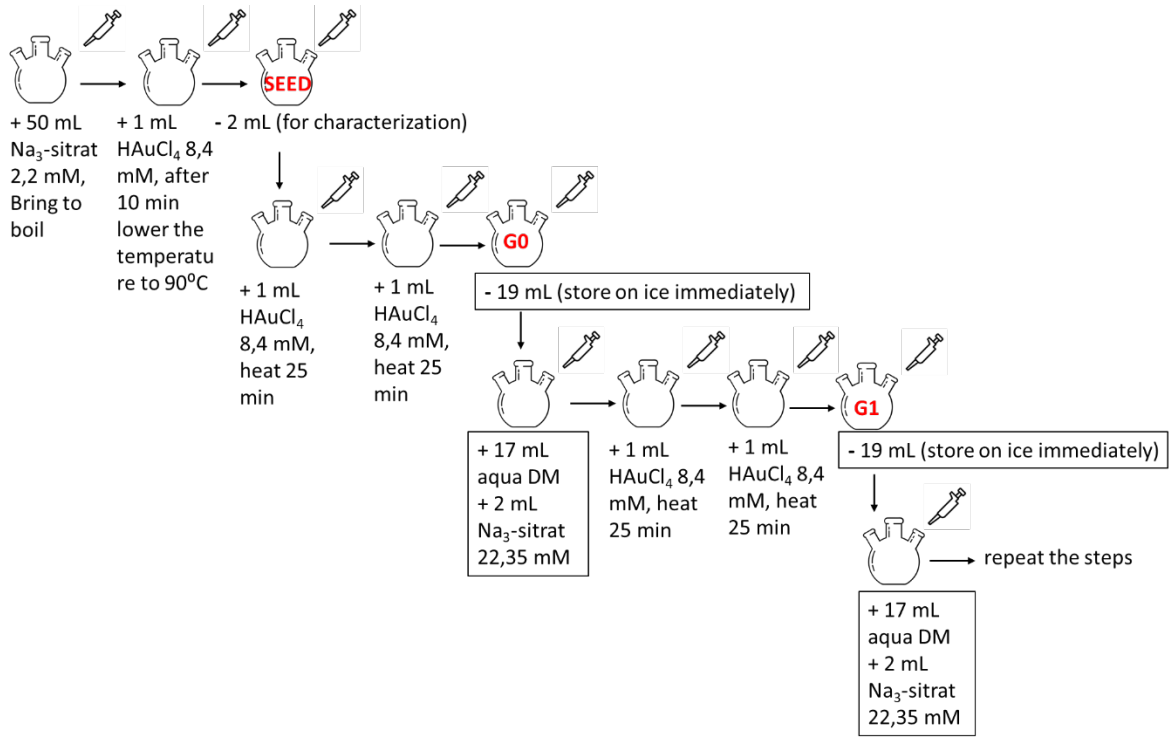

Figure S1 Diagram of gold nanoparticle synthesis.

Table S1 Economic Comparison of Gold Nanoparticle Production to Commercial Gold Nanoparticles.

Gold nanoparticle(s)	Components	Price (USD)	Price/mL (USD)
Commercial (Brand: Nanosphere Bioready) Size: 20 nm Volume: 5 mL OD: 20 (equivalent to an OD of 1.5 of 67 mL)	Product price, Shipping cost, Tax	80	1.2
Brand: Nanoflow (commercial) Size: 40 nm Volume: 50 mL OD: 1.8 (equivalent to an OD of 1.5 of 60 mL)	Product price, Shipping cost, Tax	485	8.1
Synthesized nanoparticles Size: 20 nm volume: 20 mL OD: 1,5 (This does not include the costs of purification)	Chemicals, Energy, manpower	1.54	0.077

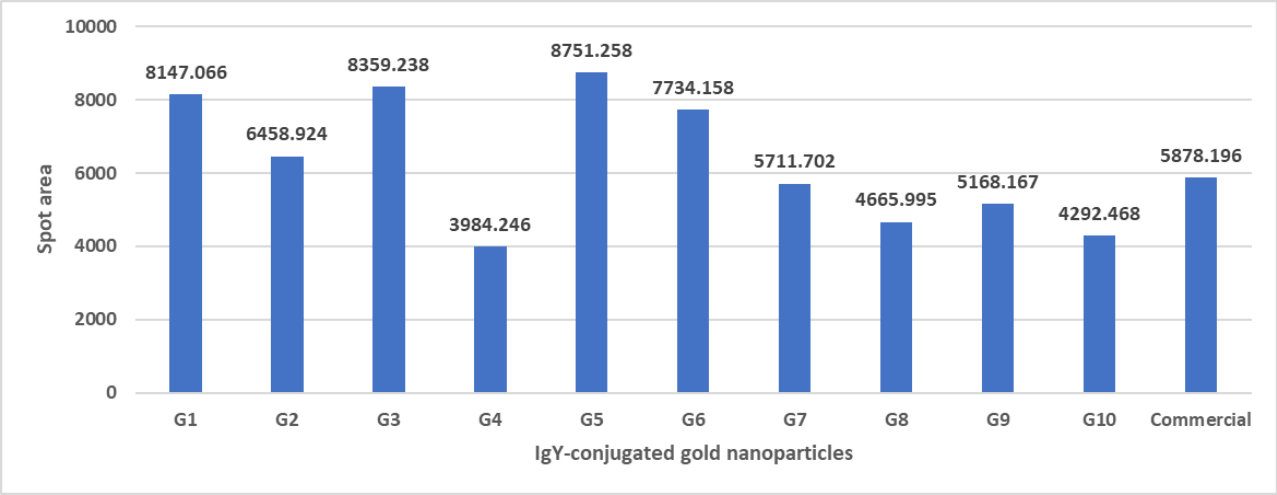

Figure S2 Sensitivity of various IgY-conjugated gold nanoparticles to the N-SARS-CoV-2 protein was indicated by the area of the spots in the half-strip test. The spot areas were calculated by using ImageJ.